Progress In Electromagnetics Research Letters, Vol. 98, 139–144, 2021

A Compact Negative Group Delay Circuit Topology Based on Asymmetric Coplanar Striplines and Double-Sided Parallel Striplines

Zhongbao Wang*, Yu Bai, Yuwei Meng, Shaojun Fang, and Hongmei Liu

Abstract—An innovative negative group delay (NGD) circuit topology based on asymmetric coplanar striplines (ACPSs) and double-sided parallel striplines (DSPSs) is proposed. The original NGD circuit topology consists of two sections of ACPS, one section of open-circuited DSPS, a connecting hole, and a group of grounding holes. The NGD characteristic is achieved by the open-circuited DSPSs combined with the connecting hole. To verify the proposed NGD circuit topology, a prototype is designed, fabricated, and measured. From the measured results, an NGD time of −2.42 ns at the center frequency of 1.577 GHz is obtained with an NGD bandwidth of 36 MHz (1.561–1.597 GHz). The insertion loss is less than 4.75 dB with the return loss larger than 11.7 dB in the NGD band.

1. INTRODUCTION

Group delay (GD) distortion is one of the challenging issues in a circuit or system, which may cause the inter-symbol interference of wideband communication systems and the pseudo-range error of global navigation satellite systems (GNSSs). To address these issues, negative group delay circuit (NGDC) has been applied to compensate the GD distortion [1], enhance the bandwidth of analog feedback amplifier [2], increase the efficiency of feed-forward linearization amplifier [3], minimize the beam-squint in phased array antenna [4], realize linear-phase bandpass filter [5], and design wideband phase shifter [6].

Traditional NGDCs are realized by RLC resonators or transmission lines loaded with resistors [7–9]. However, they always have large insertion loss (IL) and require lumped components. Usually, these lumped components only have some standard values, which limit the flexibility of design. To solve this problem, several novel low-loss NGDCs without lumped components have been proposed [10–15]. In [10], a coupled line coupler-based NGDC without requiring resistors was proposed by using the isolated and coupled-accesses connected in a feedback loop through a lossy interconnect line. After that, an NGDC based on a coupling matrix with finite unloaded quality factor resonators was proposed in [11]. Recently, an NGDC was designed by using one section of coupled lines with open- and stub-loaded terminations [12]. In [13], a turtle-shaped NGDC was proposed, which comprised two different-length transmission lines interconnecting two identical coupled lines. In [14], a low-loss NGDC consisted of two identical coupled-lines and three identical transmission lines. In [15], a diakoptics modeling of flying bird-shaped NGDC was developed. However, the use of the coupled-lines made the theoretical analysis of these NGDCs complicated.

In this paper, a compact NGDC topology based on asymmetric coplanar striplines (ACPSs) and double-sided parallel striplines (DSPSs) is proposed. The proposed NGDC is composed of two sections of ACPS, an open-circuited DSPS, a connecting hole, and a group of grounding holes. The negative group delay (NGD) characteristic is achieved by the open-circuited DSPS combined with the connecting hole. The analysis and results of the proposed NGDC are given and discussed.

Received 30 May 2021, Accepted 30 June 2021, Scheduled 1 July 2021
* Corresponding author: Zhongbao Wang (wangzb@dlmu.edu.cn).
The authors are with the School of Information Science and Technology, Dalian Maritime University, Dalian, Liaoning 116026, China.

2. DESIGN OF THE PROPOSED NGDC

Figure 1 shows the proposed NGDC topology, which consists of two ACPSs, an open-circuited DSPS, a connecting hole, and a group of grounding via holes. Two ACPSs connected with input and output ports are printed on the top and bottom sides of a substrate, respectively. The ground planes of ACPSs are connected by a group of via holes. The top and bottom strips of the open-circuited DSPS are connected to the top and bottom ACPSs, respectively. Furthermore, a connecting hole is also connected to the top and bottom strips of the open-circuited DSPS, as shown in Fig. 1. The NGD characteristic of the proposed NGDC is generated by the open-circuited DSPS combined with the connecting hole, which is equivalent to a parallel RLC resonator in series with input and output ACPSs. Therefore, the NGD time and operation frequency are mainly controlled by changing the length and width of the open-circuited DSPS (i.e., the capacitance and resistance of the parallel RLC resonator) and the diameter of the connecting hole (i.e., the inductance of the parallel RLC resonator).

Figure 2 gives the effects of the open-circuited DSPS on the performances of the proposed NGDC. When the length of the open-circuited DSPS L_d is increased from 23.6 to 24.6 mm, the NGD center frequency is decreased, and NGD absolute value and IL at the center frequency are slightly decreased.

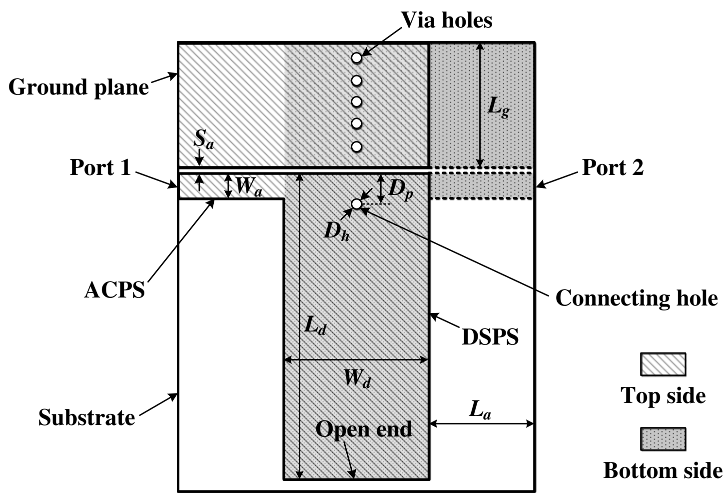

Figure 1. Configuration of the proposed NGDC.

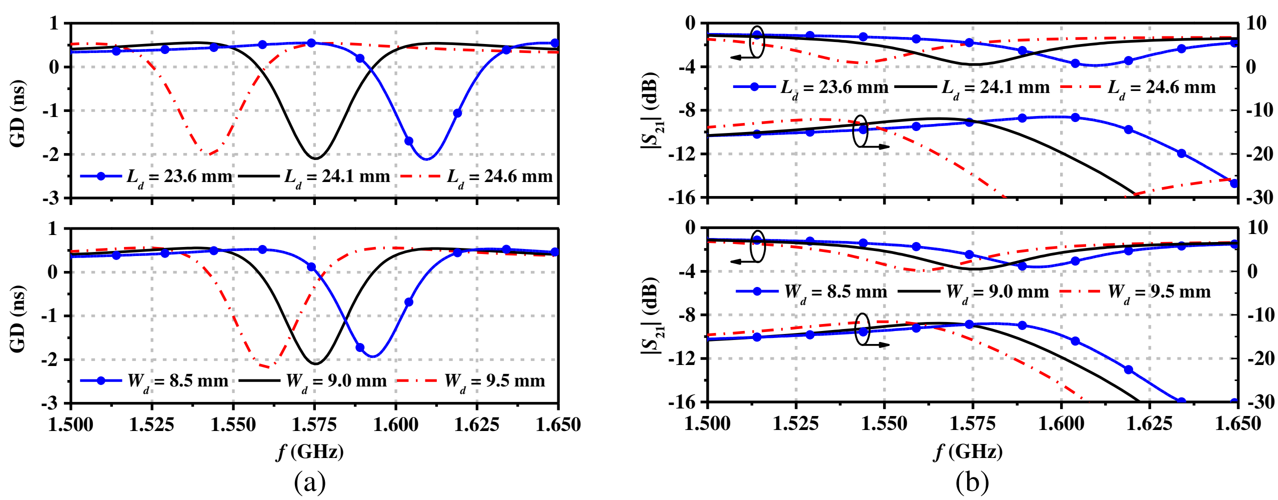

Figure 2. Effect of L_d and W_d on the performances of the proposed NGDC. (a) GD. (b) S-parameters.

Contrary to L_d, the NGD absolute value and IL at the center frequency are slightly increased by increasing the width of the open-circuited DSPS W_d from 8.5 to 9.5 mm. Also, the NGD center frequency is decreased by increasing W_d. Furthermore, the open-circuited DSPS has a slight effect on the $|S_{11}|$ at the NGD center frequency.

Figure 3 shows the effects of the connecting hole on the performances of the proposed NGDC. When the diameter of the connecting hole D_h is increased from 0.7 to 1.3 mm, the NGD center frequency is increased. Meanwhile, NGD absolute value and IL at the center frequency are decreased. When D_h is less than 0.7 mm, $|S_{11}|$ at the NGD center frequency will be greater than -10 dB. As shown in Fig. 3, when D_p is increased from 2.5 to 3.5 mm, the NGD center frequency is increased. D_p has a negligible effect on the NGD absolute value, IL, and $|S_{11}|$ at the center frequency.

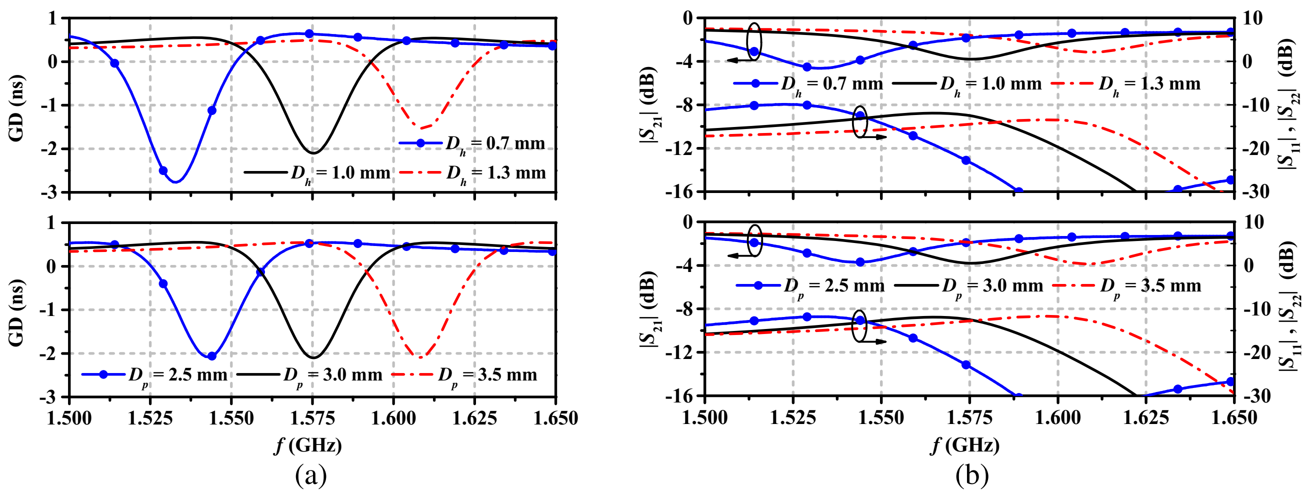

Figure 3. Effect of D_h and D_p on the performances of the proposed NGDC. (a) GD. (b) S-parameters.

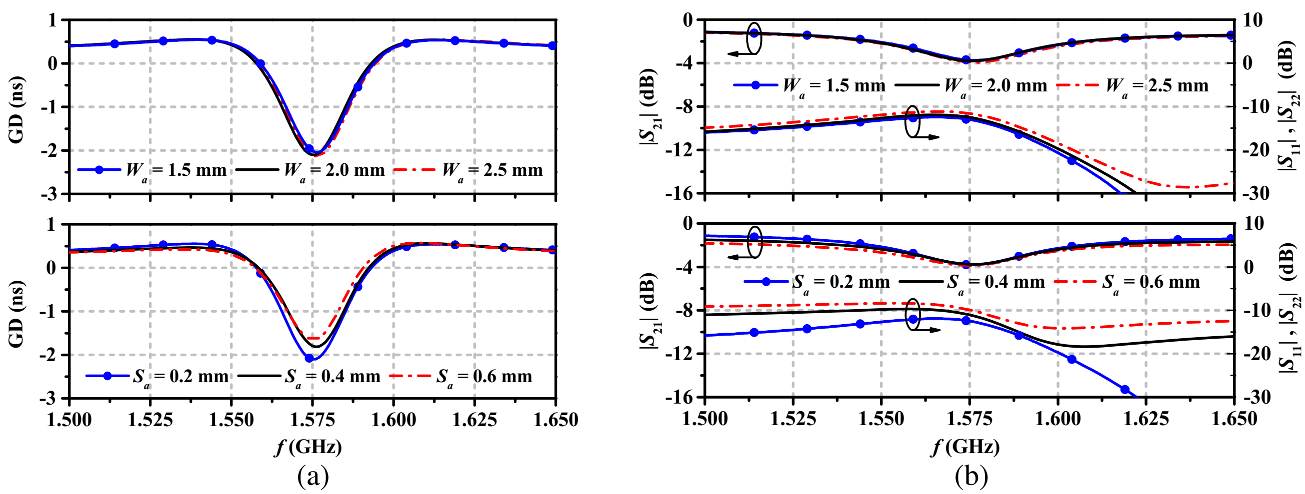

Figure 4. Effect of W_a and S_a on the performances of the proposed NGDC. (a) GD. (b) S-parameters.

Figure 4 gives the effects of ACPS on the performances of the proposed NGDC. When the strip width of the ACPS W_a is increased from 1.5 to 2.5 mm, $|S_{11}|$ is degraded with a negligible change of GD and IL. As shown in Fig. 4, when the slot width of ACPS S_a is increased from 0.2 to 0.6 mm, the NGD absolute value at the center frequency is decreased with degradation of $|S_{11}|$. Thus, there is a compromise between impedance matching and fabricating difficulty.

Based on the foregoing analysis, the following procedures are suggested to design the proposed NGDC.

1) Determine the NGD time and center frequency according to the design requirements. Obtain the values of relative dielectric constant ε_r and thickness h of the substrate.

2) Select a proper width of DSPS W_d referring to Fig. 2. Then calculate the length of DSPS L_d to be about $\lambda_g/4$, where the guided wavelength λ_g of DSPS is the same as that of a microstrip line with the substrate thickness $h/2$ [16].

3) Choose a proper diameter of the connecting hole D_h based on the desired NGD time (Fig. 3).

4) Select a slot width of ACPS S_a according to the fabricating technology (Fig. 4).

5) Adjust S_a and W_a in a full-wave electromagnetic simulator to achieve the impedance matching, referring to Fig. 4.

6) Change D_h according to Fig. 3 to obtain the desired NGD time.

7) Tune D_p referring to Fig. 3 to achieve the needed center frequency.

3. IMPLEMENTATION AND PERFORMANCE

To validate the proposed topology, an NGDC prototype is designed and implemented on a 1.6 mm-thick substrate with a relative dielectric constant of 4.4 and loss tangent of 0.02. The HFSS EM software is used to obtain the optimized dimensions. The dimensions of the NGDC are found and implemented as follows: $W_d = 9.0$ mm, $L_d = 24.1$ mm, $D_h = 1.0$ mm, $D_p = 3.0$ mm, $W_a = 2.0$ mm, $S_a = 0.2$ mm, $L_a = 8.5$ mm, and $L_g = 11.8$ mm. Photographs of the fabricated NGDC are shown in Fig. 5. The circuit

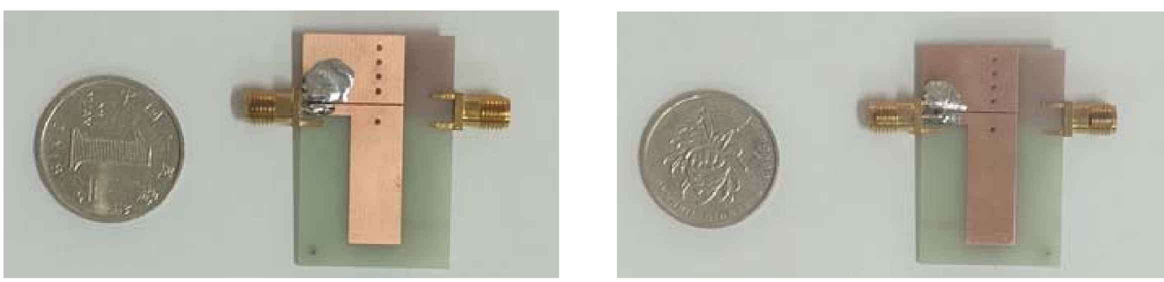

(a) (b)

Figure 5. Photographs of the fabricated NGDC. (a) Top view. (b) Bottom view.

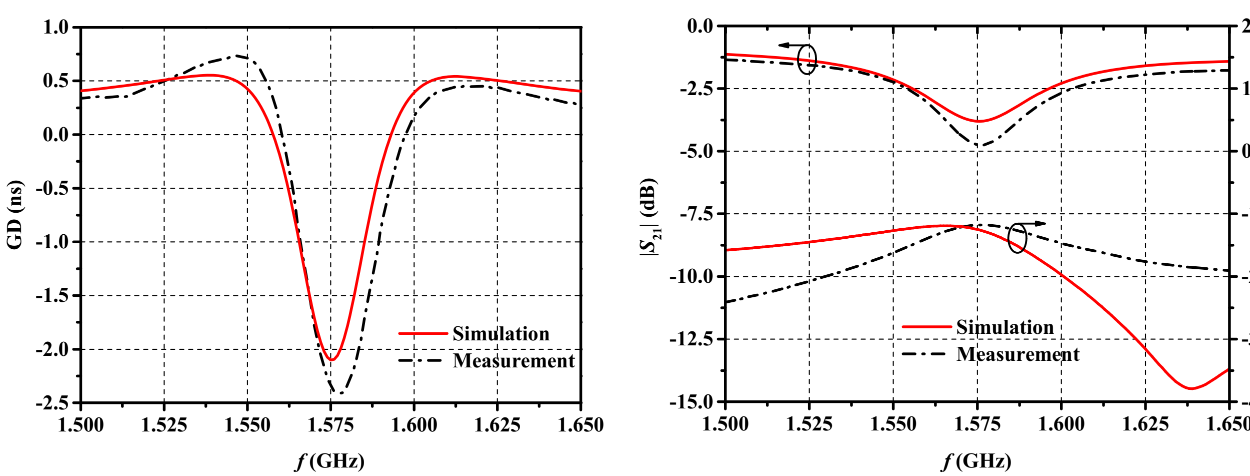

(a) (b)

Figure 6. Simulated and measured results of the proposed NGDC. (a) GD. (b) S-parameters.

size of the prototype is 40 mm × 26 mm (around $0.38\lambda_g \times 0.25\lambda_g$, where λ_g is the guided wavelength of 50-Ω transmission line at the center frequency). The fabricated NGDC is measured with an Agilent N5230A network analyzer.

Figure 6 gives the simulated and measured results of the proposed NGDC. As shown in Fig. 6(a), the measured NGD time is −2.42 ns at the center frequency of 1.577 GHz. The fractional bandwidth (FBW) for GD less than 0 ns is 2.28% (1.561–1.597 GHz). In the NGD band, the measured IL and return loss (RL) are better than 4.75 dB and 11.7 dB, respectively. There are some discrepancies between the simulated and measured results, which are mainly due to inaccurate dielectric constant and loss of the used FR4 substrate in the prototype and fabrication tolerance. Table 1 shows the comparison of the proposed NGDC with previous designs. Compared with [7–15], the proposed circuit without using the coupled-lines and lumped resistors has a simple and flexible design with a moderate IL, circuit size, and figure of merit (FOM), where the FOM is defined as

$$\mathrm{FOM} = \left|\mathrm{NGD}\left(f_0\right)\right| \times \mathrm{BW_{NGD}} \times \left|S_{21}\left(f_0\right)\right|. \tag{1}$$

Table 1. Performance comparison.

Ref.	f_0 (GHz)	NGD (ns)	IL (dB)	RL (dB)	NGD FBW (%)	FOM	Size ($\lambda_g \times \lambda_g$)	Use of resistor	Use of coupled-lines
[7]	1.016	−2.09	18.1	33.0	14.2	0.0375	0.41 × 0.41	Y	Y
[8]	3.450	−4.60	20.5	33.7	3.48	0.0521	0.33 × 0.29	Y	Y
[9]	1.570	−8.75	20.5	32.0	3.82	0.0495	0.39 × 0.19	Y	Y
[10]	1.260	−2.20	2.40	14.0	1.59	0.0334	0.63 × 0.28	N	Y
[11]	2.140	−1.03	3.82	12.0	2.80	0.0398	0.74 × 0.40	N	Y
[12]	1.528	−2.89	2.91	11.9	1.57	0.0496	0.38 × 0.30	N	Y
[13]	1.970	−1.00	2.20	14.0	1.02	0.0155	0.31 × 1.25	N	Y
[14]	1.890	−1.00	1.70	15.0	1.06	0.0164	1.06 × 0.51	N	Y
[15]	1.150	−2.20	1.93	13.0	1.30	0.0264	0.44 × 0.15	N	Y
This work	1.579	−2.42	4.75	11.7	2.28	0.0504	0.38 × 0.25	N	N

4. CONCLUSIONS

In this paper, a compact NGDC topology using ACPSs and DSPSs has been presented. Based on the parametric analysis, the NGD characteristic of the proposed circuit is mainly controlled by the open-circuited DSPS combined with the connecting hole. The proposed NGDC topology without the use of coupled lines and lumped components has a simple and flexible design. Its IL and size are small. So it can be applied to various microwave communication and GNSS systems for performance enhancement.

ACKNOWLEDGMENT

This work was supported by the National Natural Science Foundation of China (Nos. 61871417 and 51809030), the LiaoNing Revitalization Talents Program (Nos. XLYC2007024 and XLYC2007067), the Natural Science Foundation of Liaoning Province (Nos. 2019-MS-024 and 2020-MS-127), and the Fundamental Research Funds for the Central Universities (Nos. 3132021234 and 3132021231).

REFERENCES

1. Ravelo, B., "Recovery of microwave-digital signal integrity with NGD circuits," *Photon. Optoelectron.*, Vol. 2, No. 1, 8–16, Jan. 2013.

2. Choi, H., Y. Jeong, C. D. Kim, and J. S. Kenney, "Bandwidth enhancement of an analog feedback amplifier by employing a negative group delay circuit," *Progress In Electromagnetics Research*, Vol. 105, 253–272, 2010.
3. Choi, H., Y. Jeong, C. D. Kim, and J. S. Kenney, "Efficiency enhancement of feedforward amplifiers by employing a negative group-delay circuit," *IEEE Trans. Microwave Theory Tech.*, Vol. 58, No. 5, 1116–1125, May 2010.
4. Mirzaei, H. and G. V. Eleftheriades, "Arbitrary-angle squint-free beamforming in series-fed antenna arrays using non-foster elements synthesized by negative-group-delay networks," *IEEE Trans. Antennas Propag.*, Vol. 63, No. 5, 1997–2010, May 2015.
5. Shao, T., Z. Wang, S. Fang, H. Liu, and Z. N. Chen, "A full-passband linear-phase band-pass filter equalized with negative group delay circuits," *IEEE Access*, Vol. 8, 43336–43343, 2020.
6. He, L., W. Li, J. Hu, and Y. Xu, "A 24-GHz source-degenerated tunable delay shifter with negative group delay compensation," *IEEE Microwave Wireless Compon. Lett.*, Vol. 28, No. 8, 687–689, Aug. 2018.
7. Wang, Z., Y. Cao, T. Shao, S. Fang, and Y. Liu, "A negative group delay microwave circuit based on signal interference techniques," *IEEE Microwave Wireless Compon. Lett.*, Vol. 28, No. 4, 290–292, Apr. 2018.
8. Xiao, J. K., Q. F. Wang, and J. G. Ma, "Matched NGD circuit with resistor-connected coupled lines," *Electron. Lett.*, Vol. 55, No. 16, 903–905, Aug. 2019.
9. Shao, T., Z. Wang, S. Fang, H. Liu, and S. Fu, "A compact transmission-line self-matched negative group delay microwave circuit," *IEEE Access*, Vol. 5, 22836–22843, Nov. 2017.
10. Ravelo, B., "Theory of coupled line coupler-based negative group delay microwave circuit," *IEEE Trans. Microwave Theory Tech.*, Vol. 64, No. 11, 3604–3611, 2016.
11. Chaudhary, G. and Y. Jeong, "Negative group delay phenomenon analysis using finite unloaded quality factor resonators," *Progress In Electromagnetics Research*, Vol. 156, 55–62, 2016.
12. Ravelo, B., N. Li, F. Wan, and J. Feng, "Design, modeling and synthesis of negative group delay IL-shape topology," *IEEE Access*, Vol. 7, 153900–153909, Oct. 2019.
13. Wan, F., N. Li, B. Ravelo, N. M. Murad, and W. Rahajandraibe, "NGD analysis of turtle-shape microstrip circuit," *IEEE Trans. Circuits Syst. II — Express Briefs*, Vol. 67, No. 11, 2477–2481, Nov. 2020.
14. Wan, F., N. Li, B. Ravelo, W. Rahajandraibe, and S. Lalléchère, "Design of T shape stub based negative group delay circuit," *IEEE Des. Test*, Vol. 38, No. 2, 78–88, Apr. 2021.
15. Ravelo, B., F. Wan, N. Li, Z. Xu, P. Thakur, and A. Thakur, "Diakoptics modelling applied to flying bird-shape NGD microstrip circuit," *IEEE Trans. Circuits Syst. II — Express Briefs*, Vol. 68, No. 2, 637–641, Feb. 2021.
16. Kim, S.-G. and K. Chang, "Ultrawide-band transitions and new microwave components using double-sided parallel-strip lines," *IEEE Trans. Microwave Theory Tech.*, Vol. 52, No. 9, 2148–2152, Sept. 2010.